COMMUNICATION

Ultra-highly selective biogas upgrading through porous MXenes†

Received 00th April 2020,
Accepted 00th January 20xx

DOI: 10.1039/x0xx00000x

Hector Prats,[a] Hannah McAloone,[b] Francesc Viñes[a] and Francesc Illas[a*]

Two-dimensional porous MXenes with M_2C formula (M = Ti, Zr, Hf, V, Nb, Ta, Cr, Mo, and W) are proposed as very promising sorbent materials for carbon dioxide (CO_2), separation from methane (CH_4) in the critical step of biogas upgrading. Density functional theory calculations including dispersion show that MXenes present very high CO_2 uptakes and selectivities even in the most adverse working conditions.

The ever-growing concentrations of CO_2 and CH_4 greenhouse gases in the atmosphere are one of the major causes of global warming.[1] In order to satisfy the worldwide growing energy demands, one would ideally profit from clean energy sources, yet maximizing the energy profit from existing sources does also contribute combating the climate change. Among several available technologies, biogas production from anaerobic digestion of energy crops, residues, and other organic wastes is gaining interest momentum to reduce the greenhouse gas emissions, or to make the existing energy supplies greener.[2] Indeed, the biogas market is being fervently promoted in cooking, power, heat, and transportation, and is expected to increase up to 29.5 Gigawatts by 2022.[3] Raw biogas consists mainly of 50-75% (v/v) CH_4 mixed with 25-50% (v/v) CO_2.[4] However, the use of biogas as fuel requires a higher CH_4 purity. Therefore, biogas upgrading to biomethane is important to increase the calorific value and to reduce unwanted components, potentially harmful to the utilisation systems,[5] which makes this process one of the most appealing and challenging ones in bioenergy industry.[3]

Among the different upgrading technologies, pressure swing adsorption (PSA) using porous solid materials has become very promising because of the compactness of the equipment, the low capital investment cost, and the safety and simplicity of the operation.[6,7] Moreover, this technology can be very energy-efficient when a suited sorbent material is utilized.[3,6] To this end, solid sorbents with a high CO_2 selectivity at standard temperature/pressure *operando* conditions, with high specific surface areas at the same time, *i.e.* high gas adsorption capacities —*a.k.a.* CO_2 uptake—, are both needed and sought. Here we present compelling evidence of the ultrahigh CO_2 uptake over CH_4 on a family of two-dimensional (2D) materials, so-called MXenes, based on accurate first-principles computational estimates of the adsorption and desorption rates of CO_2 and CH_4 on them.

The computational screening of effective solid sorbents by first-principles, combined with a statistical thermodynamics approach, has proven to be a very powerful, predictive tool to accurately estimate the different interaction of a given material with CO_2 and CH_4, and is used to deliver useful estimates of selectivities and adsorption capacities when posing new materials for biogas upgrading.[8] Presently, density functional theory (DFT) simulations including dispersive forces are the most widely-used approach to compute adsorptive properties of solid materials, being the best balance between accuracy and efficiency for relatively large simulated systems, especially useful to describe CH_4 and CO_2 interactions with a plethora of compounds, including transition metals (TMs),[9,10] transition metal carbides (TMCs),[8,11,12] zeolites,[13] metal-organic frameworks (MOFs),[14] nanoporous carbons,[15] and periodic mesoporous phenylene-silica (MPOs).[16]

Recently, Morales-Garcia *et al.* computationally assessed the CO_2 capture on most stable and featured (0001) surfaces of MXenes,[17] a novel family of two-dimensional (2D) transition metal carbides and nitrides, composed of stacked close-packed layers of early TMs with sandwiched layers of carbon or nitrogen. Regarding CO_2 capacity, from a conservative viewpoint, it was predicted that three-layered MXenes with M_2C stoichiometry display uptakes ranging from ~2.3 to ~8 mol CO_2 kg^{-1} for periods IV-VI TM MXenes, surpassing earlier values on zeolites —3.36 and 3.96 mol CO_2 kg^{-1} for Ca-X[18] and 13X[19] respectively— and reduced graphene oxide derivatives —3.96 mol CO_2 kg^{-1} for a-RGO-950[20]— unfolding the high potential of these 2D materials for CO_2 storage. Subsequent work revealed that the CO_2 interaction is not much dependent on the MXene thickness.[21] Precisely, the TMC(111) surface, theoretically studied by Quesne *et al.*[12] can be regarded as the limit for thick MXenes and, on the other hand, these thick MXenes[21] provide a physical realization of these surfaces that, due to their high surface energy, are difficult to prepare in

[a] *Departament de Ciència de Materials i Química Física & Institut de Química Teòrica i Computacional (IQTCUB), Universitat de Barcelona, c/ Martí i Franqués 1-11, 08028 Barcelona, Spain.*
[b] *Department of Chemistry, University of Warwick, Coventry, CV4 7AL.*

† Electronic supplementary information (ESI) available: Computational details, parameters used in the HT/HR model, estimation of average equilibrium constants, and CH_4 adsorption energies. See DOI: 10.1039/x0xx00000x

experiments. Interestingly, recent experiments by Persson *et al.*[22] validated the DFT predictions by reporting an even higher CO_2 uptake of ~12 mol CO_2 kg^{-1} for Ti_3C_2.

Such 2D MXenes, with high surface areas in the range of 250-1000 m^2g^{-1}, are latest additions to the 2D world,[23,24] and have already been tested for a wide variety of applications, including energy storage,[25] water purification,[26] and catalysis,[27] to name a few. MXenes have been recently regarded as nanomembranes, suited to ultra-highly separate H_2 from CO_2, with selectivities over 440,[28] although the MXene surface functionalization with borate or imine moieties is regarded as a way of tuning the gas permeation and selectivity, even to the point of reversing the preference towards CO_2, with a selectivity over H_2 of ~17. Such functionalized MXenes can be used for CO_2 separation from CH_4, with selectivities of ~15. Such a selectivity is slightly better than that featured by porous graphene, with values of 4-12,[29,30] but still sensibly smaller than sulfone-functionalized graphene oxide, with a reported value of 75.[31] Here, motivated by the previous results from Morales-Garcia *et al.*[17] on the strong interaction between pristine MXenes and CO_2, we show, by DFT-based simulations of CO_2 and CH_4 adsorption and desorption rates, that such materials can yield ultra-high selectivities of CO_2 adsorption *vs.* CH_4, well above 10^{10}, even up to the order of that obtained by porous graphene separating H_2 from CH_4, being 10^{23}.

Briefly, the DFT calculations have been carried out using the Vienna *ab initio* simulation package (VASP) code,[32] employing the Perdew-Burke-Ernzerhof (PBE) exchange-correlation functional.[33] The dispersive forces, crucial to correctly describe the weak physisorption of methane, have been described through the Grimme D3 approach.[34] Spin-polarization has been shown to be important for Cr_2C, Ti_2C and Zr_2C, yet negligible on the other MXenes. Further computational details are found in the electronic supplementary information (ESI). For the sake of clarity, we note here that favourable adsorption energies, E^i_{ads}, where *i* = CH_4 or CO_2, are defined negative.

Table 1 Calculated PBE-D3 E^i_{ads} including the zero-point energy term for CH_4 and CO_2 on most stable adsorption modes for all nine MXenes.

MXene	$E^{CH_4}_{ads}$	Site	$E^{CO_2}_{ads}$	Site
Ti_2C	-0.25	$C_TH_MH_C$	-3.34	$C_CO_MO_M$
Zr_2C	-0.21	$C_TH_MH_C$	-3.21	$C_CO_MO_M$
Hf_2C	-0.13	$C_TH_MH_C$/$C_TH_BH_B$/ $C_TH_CH_CH_C$	-3.36[a]	$C_CO_MO_M$
V_2C	-0.35	$C_TH_MH_C$	-2.41[a]	$C_CO_MO_M$
Nb_2C	-0.24	$C_TH_MH_C$/$C_TH_BH_B$	-2.11[a]	C_MO_B
Ta_2C	-0.25	$C_TH_MH_C$	-2.37[a]	C_M
Cr_2C	-0.31	$C_TH_MH_C$	-2.13	C_BO_B
Mo_2C	-0.38	$C_TH_MH_C$/$C_TH_BH_B$	-1.63[a]	C_MO_B
W_2C	-0.23	$H_T(H_MH_MH_M)$	-1.31[a]	$C_CO_MO_M$

[a] Values taken from Ref. 17

The CH_4 adsorption sites have been identified through an exhaustive computational screening; four non-equivalent high-symmetry surface sites have been tested on each MXene (0001) surface, namely, top and bridge sites, plus two hollow sites, either with a subsurface metal or carbon site. The interaction of CH_4 on each site has been evaluated for three different connectivities, with one, two, or three H atoms pointing toward the MXene surface.[35] Finally, two different molecular orientations have been evaluated for each site and connectivity, sampling a total of 24 conformations per MXene.

A coordination chemistry based adsorption connection labelling has been used, as earlier done for CO_2 adsorbed on such MXenes,[17] and the details are explained in the ESI. As an example, η^3-CH_4-μ^1-$C_TH_MH_C$ refers to a CH_4 molecule connecting through three atoms, η^3, and involving one MXene surface metal atom, μ^1. The three CH_4 connecting atoms are one C over a metal Top site, C_T, and two H atoms, located over Metal hollow, H_M, and Carbon hollow, H_C, sites, see Figure 1, although for simplicity the latter $C_TH_MH_C$ part is used, as it already defines the adsorptive conformation. For the adsorption modes with only one H atom pointing to the surface, the position of the other 3 H atoms are also indicated in parenthesis to distinguish between different orientations. A complete list of sampled sites and their corresponding $E^{CH_4}_{ads}$ values is found in Figure S1 and Tables S2-S4 of the ESI. The obtained results for CH_4, listed in Table 1, range from -0.03 to -0.38 eV, being $C_TH_MH_C$ and $C_TH_BH_B$ the most favourable adsorption modes in all MXenes but W_2C, where most favourable is $H_T(H_MH_MH_M)$. Table 1 encompasses the most-stable CO_2 adsorption energy values, taken from a recent work using the same computational setup, yet here, for consistency, considering spin-polarization for Cr_2C, Ti_2C, and Zr_2C MXenes. The final picture of CO_2 capture on MXenes is kept, with $E^{CO_2}_{ads}$ from -2.11 to -3.36 eV, and most stable sites shown in Figure 1.

The direct comparison of E^i_{ads} suggests a very high CO_2 selectivity over CH_4 for all MXenes, specially for group IV MXenes, given the small adsorption energies for CH_4, ranging from -0.13 to -0.25 eV, compared to those of CO_2, 13–26 times larger, in the order of *ca.* -3.3 eV. The smallest difference in E_{ads} is found for W_2C, with an $E^{CO_2}_{ads}$ of -1.31 eV, only ~6 times larger than that for CH_4. Note also that, because methane

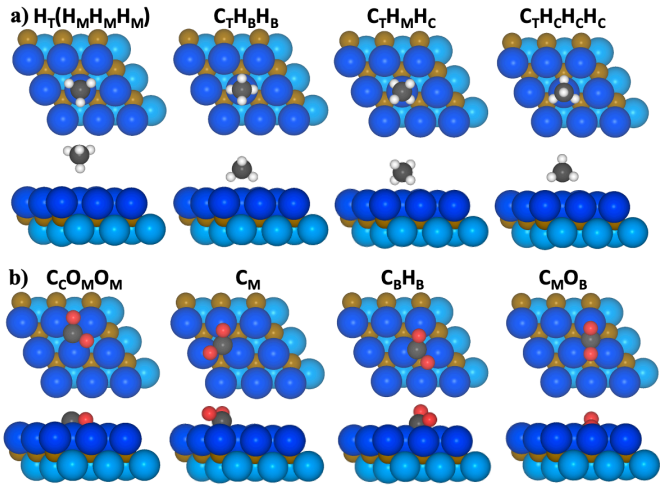

Fig 1 Top (top image) and side (bottom image) views of the most stable adsorption modes of CH_4 and CO_2 on MXenes. C and O atoms for adsorbates are represented by gray and red spheres, C atoms in MXene are shown as brown spheres, and metal atoms are represented by dark (top layer) and light (bottom layer) blue spheres.

interacts in a rather similar weak way on all investigated MXenes, see Table 1, mostly due to the role of dispersive forces, which are rather surface insensitive. Thus, the selectivity differences arise from their interaction with CO_2, ruled by the number of d electrons the MXene metal has.[17]

The selectivity of CO_2 over CH_4 at low coverage and equal gases partial pressures, S_{CO_2/CH_4}, which is dependent of temperature, T, and gases partial pressure, p_i, can be estimated from equilibrium constants for adsorption, K_i, as:

$$S_{CO_2/CH_4} = \frac{K_{CO_2}}{K_{CH_4}} = \frac{k_{ads}^{CO_2}/k_{des}^{CO_2}}{k_{ads}^{CH_4}/k_{des}^{CH_4}} = \frac{e^{-\Delta G_{ads}^{CO_2}/k_B T}}{e^{-\Delta G_{ads}^{CH_4}/k_B T}} \quad (1),$$

where k_B is the Boltzmann constant, and ΔG_{ads}^{i} the T- and p_i-dependent adsorption free energies of i species, computed as:

$$\Delta G_{ads}^{i} = E_{ads}^{i} + G_{ads}^{i,cont} - G_{gas}^{i,cont} \quad (2),$$

where $G_{ads}^{i,cont}$ is the T-dependent contribution to the free energy of i species when adsorbed on the MXene, and $G_{gas}^{i,cont}$ that T- and p_i-dependent of the gas-phase species. Specifically, free energy corrections for gas-phase species are calculated in the ideal gas approximation. For adsorbed species, $G_{ads}^{CO_2,cont}$ has been computed with the harmonic oscillator (HO) model for all degrees of freedom, being a suited model for chemisorbed CO_2. Conversely, the HO model has been shown to fail when estimating entropies for physisorbed molecules featuring low rotational and diffusion barriers, *e.g.* CH_4, as recently duly emphasized by Sprowl *et al.*,[36] who suggest to estimate entropies within the hindered translator/hindered rotor (HT/HR) model, which considerable improves the description of closed-shell molecules such as CH_4 and propane. This has been applied for $G_{ads}^{CH_4,cont}$, considering two degrees of freedom as hindered translations parallel to the surface, and one degree of freedom as a hindered rotation around an axis perpendicular to the surface, whereas the remaining degrees of freedom are treated as HO vibrations. The needed diffusion and rotation energy barriers have been gained through the climbing-image nudged elastic band (*CI-NEB*) method,[37] see Table S1 of the ESI. The free energy contributions have been computed using the ASE thermochemistry module.[38] For CH_4, different close-in-energy physisorbed situations coexist. Consequently, the macroscopic K_{CH_4} is superimposed from these contributions, and we calculated an average value among all these adsorption modes, see further details in the ESI.

The calculated selectivity values steaming from Eq. 1 are shown, in the 100−1000 K temperature range, in Figure 2a. All MXenes feature extremely high selectivities at room temperatures, mostly maintained even at medium temperature of ~700 K. Hf_2C MXene features the highest selectivity, overwhelmingly predicted to be $\sim 10^{49}$ at room temperature —300 K—, maintained to $\sim 10^{10}$ at 1000 K. On the other hand, W_2C is the least selective MXene, but still with a very high selectivity of 10^{13} at 300 K which, in theory, would ensure a biogas CH_4 enrichment of nearly 100%. The CO_2/CH_4 MXenes selectivity decays as Group IV > Group V > Group VI, with the sole exception of Cr_2C, which, being Group VI behaves as Group V.

To better assess the MXenes biogas upgrading performance we calculated the adsorption and desorption rate constants k_{ads}^{i} and k_{des}^{i}, respectively, for both i species, on the just-mentioned highest and lowest selective MXenes. The molecular adsorption has been assumed to be non-activated, and so, in accordance to kinetic gas theory, the adsorption rate constant can be estimated as

$$k_{ads}^{i} = \frac{S p_i A_{site}}{\sqrt{2\pi m_i k_B T}} \quad (3),$$

where m_i is the molecular mass, A_{site} the adsorption site area, and S the sticking coefficient.[39] Finally, the desorption of adsorbed molecules represents the adsorption reversed process, and so has to fulfil;

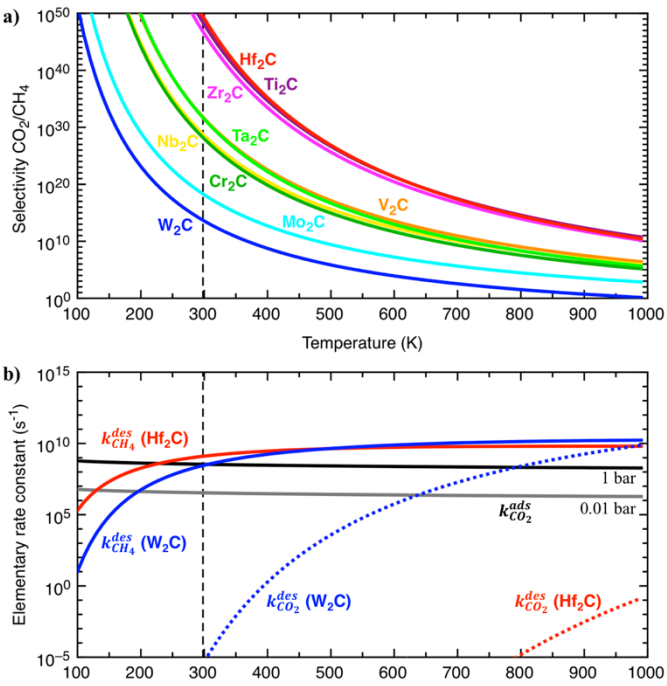

Fig. 2 (a) Calculated CO_2 over CH_4 selectivity values for on all nine MXenes as a function of the T, considering equal pressures of 1 bar for both species, and (b) adsorption and desorption rate constants for W_2C and Hf_2C limit cases. Notice that adsorption rates are considered for low (0.01 bar) and normal (1 bar) partial pressures, and that the lines basically superimpose for both CO_2 and CH_4.

$$k_{des}^{i} = \frac{k_{ads}^{i}}{K_i} = \frac{k_{ads}^{i}}{e^{-\Delta G_{ads}^{i}/k_B T}} \quad (4).$$

The results in Figure 2b show that, for Hf_2C, $k_{ads}^{CO_2} \gg k_{des}^{CO_2}$ in all the explored temperature range, suggesting a preferred CO_2 uptake even at 1000 K. In W_2C case, this preference is maintained only up to 750 K at 1 bar of gases pressures —600 K for 0.01 bar pressures. Above this temperature, the CO_2 desorption rate would be higher than that for the adsorption, and, therefore, the selectivity would become irrelevant as the MXene surface would tend to get clean.

Note that present estimations are given assuming a series of approximations, and their effect on the overall picture should be regarded. For instance, the adsorption energies are

considered at the initial stages of molecular capture —*i.e.* low coverage regime— where adsorbate lateral interactions can be disregarded. Notice that lateral interactions for CO_2 at medium coverages are not repulsive according to the literature, as seen on Ni[40] or α-Mo_2C.[41] Thus, even when there might be discrepancies between actual and estimated ideal selectivities, the adsorption strength differences between CO_2 and CH_4 are acute enough so to guarantee ultra-high selectivities compared to current most selective materials. Notice that the under- or overestimation of E_{ads}^{i} by the PBE-D3 approach could be another influential source on the selectivity accuracy, although the artificial strengthening of $E_{ads}^{CH_4}$ and weakening of $E_{ads}^{CO_2}$ bond strengths, both by 0.2 eV, considered the upper limit of DFT accuracy, still maintains the high-selectivity values well within 10^7-10^{43} at 300 K, see Figure S2a in the ESI. Aside, the enrichment of CH_4 above analytical purity grade, *i.e.* 99.99%, is addressed considering a mixture with solely 0.01% of CO2 in Figure S2b. In such an extreme situation, the selectivities are kept in between 10^{10} and 10^{45} at 300 K. Altogether, these sensitivity values not only reinforce the statement of ultra-high selectivity biogas upgrading by MXenes, but also show that these materials could be used for upgrading low CO_2 content CO_2/CH_4 mixtures such as natural gas.

Hence, present values for MXenes surpass previous results for other formerly materials described in the literature, including sulfone-functionalized graphene oxide, with a reported value of 75,[31] or the highest reported value of $\sim 10^3$ at 0.5 bar and 293 K,[42] obtained on the $|Na_{10.2}KCs_{0.8}|$-LTA zeolite. Indeed, the forecasted MXene values are order of magnitudes larger than the corresponding bulk TMC reported values;[8] for instance, compare the room temperature value of $\sim 10^{18}$ for HfC, compared to the present $\sim 10^{49}$ value on Hf_2C. This difference underscores the higher chemical activity of carbide MXenes compared to TMCs, particularly towards CO_2. This has been proven to be the consequence of MXenes featuring (0001) surfaces, geometrically and electronically resembling the (111) ones of TMCs, which are less stable than (001), and so more chemically active.[21]

In summary, DFT PBE-D3 calculations for the interaction of CH_4 and CO_2 with most stable (0001) surfaces of nine carbide MXenes, coupled to *ab initio* thermodynamics and statistic thermodynamics rate constant estimates unfold the superior separation capabilities of such 2D materials for the selective biogas upgrading. It is worth pointing out that a recent DFT-based study[17] predicted very high gravimetric CO_2 capacities for all these MXenes, a prediction that was even experimentally overpassed as described in the recent work of Persson et al.[22], reporting a CO_2 uptake of $\sim$12 mol CO_2 kg^{-1} for Ti_3C_2. However, no information was provided regarding their selectivity in biogas mixtures. The present results predict weak CH_4 attachment energies in all MXenes, in contrast to very large CO_2 adsorption energies. Even within the DFT accuracy, the results forecast CO_2 adsorption selectivities above 10^{10} at 300 K over a CH_4/CO_2 stream of 0.01% CO_2 composition, which could be used for a practical biogas above analytic purity, with a concomitant better use of biogas energy power, and, consequently, and indirect benefit in sustainability by improving the energetic efficiency of currently use of biogas.

Conflicts of interest

There are no conflicts to declare.

Acknowledgements

This work has been supported by the Spanish MICIUN/FEDER RTI2018-095460-B-I00 and María de Maeztu MDM-2017-0767 grants and, in part, by *Generalitat de Catalunya* 2017SGR13 grant. H. Mc. A is grateful to the Erasmus program and F. I. acknowledges additional support from the 2015 ICREA Academia Award for Excellence in University Research.

Notes and references

1 Intergovernmental Panel on Climate Change, Climate Change 2014: Synthesis Report, IPCC, 1st edn, 2015.
2 P. Weiland, *Appl. Microbiol. Biotechnol*., 2010, **85**, 849.
3 R. Kapoor, P. Ghosh, M. Kumar, V. K. Vijay, *Environ. Sci. Pollut. Res*., 2019, **26**, 11631.
4 L. F. Gomez, R. Zacharia, P. Bénard and R. Chahine, *Adsorption*, 2015, **21**, 433.
5 Q. Sun, H. Li, J. Yan, L. Liu, Z. Yu and X. Yu, *Renew. Sust. Energ. Rev*., 2015, **51**, 521.
6 C. A. Grande, Biogas upgrading by pressure swing adsorption, Biofuel's Engineering Process Technology, Marco Aurélio dos Santos Bernardes, IntechOpen, DOI: 10.5772/18428, 2011.
7 R. Augelletti, M. Conti and M. C. Annesini*, J. Clean. Prod*., 2017, **140**, 1390.
8 C. Kunkel, F. Viñes and F. Illas, *ACS Appl. Energy Mater*., 2018, **1**, 43-47.
9 S. González, F. Viñes, J. F. García, Y. Erazo and F. Illas, *Surf. Sci*., 2014, **625**, 64.
10 X. Hao, Q. Wang, D. Li, R. Zhang and B. Wang, *RSC Adv*., 2014, **4**, 43004.
11 C. Kunkel, F. Viñes and F. Illas, *Energy Environ. Sci*., 2016, **9**, 141.
12 M. G. Quesne, A. Roldan, N. H. de Leeuw and C. R. A. Catlow, *Phys. Chem. Chem. Phys*., 2019, **21**, 10750.
13 J. Kim, A. Maiti, L.-C. Lin, J. K. Stolaroff, B. Smit and R. D. Aines, *Nat. Commun*., 2013, **4**, 1694.
14 Q. Yang, D. Liu, C. Zhong and J. Li, *Chem. Rev*., 2013, **113**, 8261.
15 Y. Ihm, V. R. Cooper, N. C. Gallego, C. I. Contescu and J. R. Morris, *J. Chem. Theory Comput*., 2014, **10**, 1.
16 C. Kunkel, F. Viñes, M. A. O. Lourenço, P. Ferreira, J. R. B. Gomes and F. Illas, *Chem. Phys. Lett*., 2017, **671**, 161.
17 A. Morales-García, A. Fernández-Fernández, F. Viñes and F. Illas, *J. Mater. Chem. A*, 2018, **6**, 3381-3385.
18 T.-H. Bae, M. R. Hudson, J. A. Mason, W. L. Queen, J. J. Dutton, K. Sumida, K. J. Micklash, S. S. Kaye, C. M. Brown and J. R. Long, *Energy Environ. Sci*., 2013, **6**, 128.
19 C. Chen, D.-W. Park and W.-S. Ahn, *Appl. Surf. Sci*., 2014, **292**, 63.
20 S. Chowdhury and R. Balasubramanian, *Ind. Eng. Chem. Res*., 2016, **55**, 7906.
21 Á. Morales-García, M. Mayans-Llorach, F. Viñes, F. Illas, *Phys. Chem. Chem. Phys*., 2019, **21**, 23136.
22 I. Persson, J. Halim, H. Lind, T. W. Hansen, J. B. Wagner, L.-A. Näslund, V. Darakchieva, J. Palisaitis, J. Rosen and P. O. A. Persson, *Adv. Mater.*, 2019, **31**, 1805472.

23 M. Naguib, O. Mashtalir, J. Carle, V. Presser, J. Lu, L. Hultman, Y. Gogotsi and M. W. Barsoum, *ACS Nano*, 2012, **6**, 1322.
24 B. Anasori, M. R. Lukatskaya and Y. Gogotsi, *Nat. Rev.*, 2017, **2**, 16098.
25 Y. Xie, M. Naguib, V. N. Mochalin, M. W: Barsoum, Y. Gogotsi, X. Yu, K. W. Nam, Q. Yang, A. I. Kolesnikov and P. R. C. Kent, *J. Am. Chem. Soc.*, 2014, **136**, 6385.
26 X. Xie, C. Chen, N. Zhang, Z.-R. Tang, J. Jiang and Y.-J. Xu, *Nat. Sustain.*, 2019, **2**, 856.
27 W. F. Chen, C. H. Wang, K. Sasaki, N. Marinkovis, W. Xu, J. T. Muckerman, T. Zhu and R. R. Adzic, *Energy Environ. Sci.*, 2013, **6**, 943.
28 J. Shen, G. Liu, Y. Ji, Q. Liu, L. Cheng, K. Guan, M. Zhang, G. Liu, J. Xiong, J. Yang and W. Jin, *Adv. Func. Mater.*, 2018, **28**, 1801511.
29 C. Sun and B. Bay, *Acta Phys. Chim. Sin.*, 2018, **34**, 1136.
30 B. Wen, C. Z. Sun and B. F. Bai, *Acta Phys. Chim. Sin.*, 2015, **31**, 261.
31 S. Wang, Y. Wu, N. Zhang, G. He, Q. Xin, X. Wu, H. Wu, X. Cao, M. D. Guiver and Z. Jiang, *Energy Environ. Sci.*, 2016, **9**, 3107.
32 G. Kresse and J. Furthmüller, *Phys. Rev. B.* 1996, **54**, 11169–11186
33 J. P. Perdew, K. Burke and M. Ernzerhof, *Phys. Rev. Lett.*, 1996, **77**, 3865.
34 S. Grimme, J. Antony, S. Ehrlich and S. Krieg, *J. Chem. Phys.*, 2010, **132**, 154104.
35 S. Posada-Pérez, J. R. dos Santos Politi, F. Viñes and F. Illas, *RSC Adv*., 2015, **5**, 33737.
36 L. H. Sprowl, C. T. Campbell and L. Árnadóttir, *J. Phys. Chem. C*, 2016, **120**, 9719.
37 G. Henkelman, B. P. Uberuaga, and H. Jónsson, *J. Chem. Phys.*, 2000, **113**, 9901.
38 A. H. Larsen, J. J. Mortensen, J. Blomqvist, I. E. Castelli, R. Christensen, M. Dułak, J. Friis, M. N. Groves, B. Hammer, C. Hargus, E. D. Hermes, P. C. Jennings, P. B. Jensen, J. Kermode, J. R. Kitchin, E. L. Kolsbjerg, J. Kubal, K. Kaasbjerg, S. Lysgaard, J. B. Maronsson, T. Maxson, T. Olsen, L. Pastewka, A. Peterson, C. Rostgaard, J. Schiøtz, O. Schütt, M. Strange, K. S. Thygesen, T. Vegge, L. Vilhelmsen, M. Walter, Z. Zeng and K. W. Jacobsen, *J. Phys. Condens. Matter*, 2017, **29**, 273002.
39 A. P. J. Jansen, An introduction to kinetic Monte Carlo simulations of surface reactions, Lecture Notes in Physics, vol. 856, Springer-Verlag, Heidelberg, Germany, 2012.
40 S.-G. Wang, D.-B. Cao, Y.-W. Li, J. Wang and H. Jiao, *J. Phys. Chem. B*, 2005, **109**, 18956.
41 Q. Luo, T. Wang, G. Walther, M. Beller and H. Jiao, *J. Power Sources*, 2014, **246**, 549.
42 O. Cheung, D. Wardecki, Z. Bacsik, P. Vasiliev, L. B. McCusker and N. Hedin, *Phys. Chem. Chem. Phys*., 2016, **18**, 16080.